Hindawi Publishing Corporation
EURASIP Journal on Advances in Signal Processing
Volume 2007, Article ID 36751, 12 pages
doi:10.1155/2007/36751

Research Article

Iris Recognition for Partially Occluded Images: Methodology and Sensitivity Analysis

A. Poursaberi[1] and B. N. Araabi[1,2]

[1] *Department of Electrical and Computer Engineering, Control and Intelligent Processing Center of Excellence, Faculty of Engineering, University of Tehran, P.O. Box 14395-515, Tehran, Iran*
[2] *School of Cognitive Sciences, Institute for Studies in Theoretical Physics and Mathematics, P.O. Box 19395-5746, Tehran, Iran*

Received 17 March 2005; Revised 12 January 2006; Accepted 15 March 2006

Recommended by Wilfried Philips

Accurate iris detection is a crucial part of an iris recognition system. One of the main issues in iris segmentation is coping with occlusion that happens due to eyelids and eyelashes. In the literature, some various methods have been suggested to solve the occlusion problem. In this paper, two different segmentations of iris are presented. In the first algorithm, a circle is located around the pupil with an appropriate diameter. The iris area encircled by the circular boundary is used for recognition purposes then. In the second method, again a circle is located around the pupil with a larger diameter. This time, however, only the lower part of the encircled iris area is utilized for individual recognition. Wavelet-based texture features are used in the process. Hamming and harmonic mean distance classifiers are exploited as a mixed classifier in suggested algorithm. It is observed that relying on a smaller but more reliable part of the iris, though reducing the net amount of information, improves the overall performance. Experimental results on CASIA database show that our method has a promising performance with an accuracy of 99.31%. The sensitivity of the proposed method is analyzed versus contrast, illumination, and noise as well, where lower sensitivity to all factors is observed when the lower half of the iris is used for recognition.

1. INTRODUCTION

Security and surveillance of information is becoming more and more important recently, in part due to the rapid development of information technology (IT) applications. The security not only includes the information but also contains the people who access the information. Other applications of security systems such as allowing authorized person to enter a restricted place, individual identification/verification, and so forth also cover a wide range of the market. Traditional methods for personal identification include things you can carry, such as keys, or things that you know. ID cards or keys can be lost, stolen, or duplicated. The same may happen for passwords or personal identification numbers. All kinds of these means are not very reliable. Hence, biometrics comes out to overcome these defects. Biometrics is the science of recognizing a person based on physical or behavioral characteristics. Biometrics description on who you are depends on one of any number of unique characteristics that you cannot lose or forget [1, 2]. Fingerprints, voiceprints, retinal blood vessel patterns, face, handwriting, and so forth can be substituted instead of nonbiometric methods for more safety and reliability. Among these biometric characteristics, a fingerprint needs physical contact and also can be captured or imitated. Voiceprint in a like manner can easily be stored. As a new branch of biometrics, iris recognition shows more satisfactory performance. The human iris is the annular part between the pupil and the sclera, and has distinct characteristics such as freckles, coronas, stripes, furrows, crypts, and so on. Compared with other biometric features, personal authentication based on iris recognition can attain high accuracy due to the rich texture of iris patterns [1–3]. Users of iris recognition system neither have to remember any passwords nor have any cards. Due to no requirement of touching for image capturing, this process is more convenient than the others.

Iris (as shown in Figure 1) is like a diaphragm between the pupil and the sclera and its function is to control the amount of light entering through the pupil. Iris is composed of elastic connective tissue such as trabecular meshwork. The iris begins to be formed in the third month of gestation, and the structures creating its pattern are largely complete by the eighth month. The agglomeration of pigment is formed during the first year of life, and pigmentation of the stroma occurs in the first few years [4]. The highly randomized

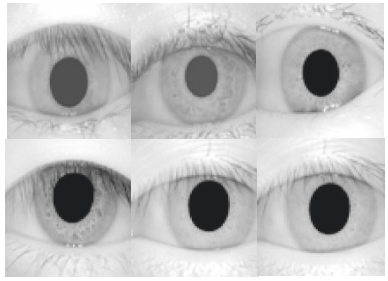

Figure 1: Samples of iris.

appearance of the iris makes its use as a biometric well recognized. Its suitability as an exceptionally accurate biometric derives from

(i) the difficulty of forging and using as an imposter person;
(ii) its intrinsic isolation and protection from the external environment;
(iii) its extremely data-rich physical structure;
(iv) its genetic properties—no two eyes are the same. The characteristic that is dependent on genetics is the pigmentation of the iris, which determines its color and determines the gross anatomy. Details of development, that are unique to each case, determine the detailed morphology;
(v) its stability over time;
(vi) the impossibility of surgically modifying it without unacceptable risk to vision and its physiological response to light, which provides a natural test against artifice.

An automatic iris recognition system includes three main steps:

(i) preprocessing such as image acquisition, iris localization, iris normalization, iris denoising, and enhancement;
(ii) iris feature extraction;
(iii) iris feature classification.

1.1. Outline of the paper

In the sequel, we first bring a history of related works in brief. An overview of our proposed algorithm is presented in Section 2, which provides a conceptual overview of our method based on an intuitive understanding for iris recognition system. Detailed descriptions of image preprocessing, feature extraction, and pattern matching for proposed algorithms are given in Sections 3, 4, and 5, respectively. In Section 6, sensitivity of our method versus contrast, illumination, and noise is analyzed. Experimental results on an iris database is reported in Section 7. Finally, the paper is concluded in Section 8, where the obtained results are summarized and the advantages of the proposed method are emphasized.

1.2. Related works

First works in iris recognition techniques were reported the late 19th century [3, 5] but most works are done in the last decade. Daugman [6, 7] used multiscale quadrature wavelets to extract texture phase structure information of the iris to generate a 2048-bit iris code and he compared the difference between a pair of iris representations by computing their Hamming distance. He showed that for identification, it is enough to have a lower than 0.34 Hamming distance with any of the iris templates in database. Ma et al. [8–10] adopted a well-known texture analysis method (multichannel Gabor filtering) to capture both global and local details in iris. They studied well Gabor filter families for feature extraction in some papers. Wildes et al. [11] with a Laplacian pyramid constructed in four different resolution levels and the normalized correlation for matching designed their system. Boles and Boashash [12] used a zero-crossing of 1D wavelet at various resolution levels to distinguish the texture of iris. Tisse et al. [13] constructed the analytic image (a combination of the original image and its Hilbert transform) to demodulate the iris texture. Lim et al. [14] used 2D Haar wavelet and quantized the 4th-level high-frequency information to form an 87-binary code length as feature vector and applied an LVQ neural network for classification. Nam et al. [15] exploited a scale-space filtering to extract unique features that use the direction of concavity of an image from an iris image. Using sharp variations points in iris was represented by Ma et al. [16]. They constructed one-dimensional intensity signal and used a particular class of wavelets with vector of position sequence of local sharp variations points as features. Sanchez-Reillo and Sanchez-Avila in [17] provided a partial implementation of the algorithm by Daugman. Also their other work on developing the method of Boles and Boashash by using different distance measures (such as Euclidean distance and Hamming distance) for matching was reported in [18]. A modified Haralick's co-occurrence method with multilayer perceptron is also introduced for extraction and classification of the iris [19, 20]. Park et al. [21] used a directional filter bank to decompose iris image into eight directional subband outputs and the normalized directional energy as features. Kumar et al. [22] utilized correlation filters to measure the consistency of iris images from the same eye. The correlation filter of each class was designed using the two-dimensional Fourier transforms of training images. Bae et al. [23] projected the iris signals onto a bank of basis vectors derived by independent component analysis and quantized the resulting projection coefficients as features. Gu et al. [24] used a multiorientation features via both spatial and frequency domains and a nonsymmetrical SVM to develop their system. They extracted features by variant fractal dimensions and steerable pyramids for orientation information.

We compare the benefits and drawbacks of some dominant works done by the others with our works in Table 1. The kind of features, matching strategy, and their results are mentioned and also we are going to overcome the common problems in most of the previous methods: occlusion.

Table 1: The comparison of methods.

Methods	Matching process	Kind of feature	Result + benefits
Daugman [6]	Hamming distance	Binary	Perfect identification + and can overcome the occlusions problem but time wasting
Wildes et al. [11]	Normalized correlation	Image	Time wasting in matching process. It can be used only in identification phase not recognition
Boles and Boashash [12]	Two dissimilarity functions: learning and classification	1D signature	Not complete recognition rate, high EER, fast process time, simple 1D feature vector, fast processing
Tan et al. [8]	Nearest feature line	1D real-valued feature vector with the length of 384	Time wasting in feature extraction, cannot cope with occlusions problem
Ma et al. [10]	Weighted Euclidean distance	1D real-valued feature vector with the length of 160	Big EER, poor recognition rate, cannot cope with occlusions problem
Ma et al. [16]	XOR operation	1D integer-valued feature vector with the length of 660	Improved last their works, good recognition rate, claims 100% correct recognition, cannot overcome the occlusions of upper eyelid and eyelashes
Sanchez-Reillo and Sanchez-Avila [17]	Euclidean and Hamming distances	1D signature	Medium classification rate, cannot cope with occlusions problem, simple 1D features
Lim et al. [14]	LVQ neural network	1D binary vector	Poor recognition rate, complicated classifier, big EER, occlusions problem
Previous [25, 26]	Hamming distance	408 and 1088 binary matrices (2 papers)	Simple low-dimensional binary features, can cope with occlusions in lower case (eyelid and eyelashes), medium recognition rate, fast processing, not engaging with edge detection
Proposed	Complex classifier (joint of Hamming distance of minimum and harmonic mean)	544 binary matrix	Not engaging with edge detection which is time wasting and not accurate as iris is not a complete circle-shape, can conquer the occlusions in both upper and lower cases, simple and short feature length, fast processing

2. AN OVERVIEW OF THE PROPOSED APPROACH

In this paper, to implement an automatic iris recognition system, we propose a new algorithm in both iris detection and feature extraction modes. Using morphological operators for pupil detection and selecting the appropriate radius around the pupil to pick the region of iris which contains the collarette—that appears as a zigzag pattern—are the main contributions of the paper. This region provides a unique textual pattern for feature extraction. Selected coefficients of 4-level and 3-level Daubechies wavelet decompositions of iris images are chosen to generate a feature vector. To save the storage space and computational time for manipulating the feature vector, we quantize each real value into binary value using merely its sign disregarding its magnitude. A typical iris recognition system includes some major steps as depicted in Figure 2. At first, an imaging system must be designed to capture a sequence of iris images from the subject in front of camera. A comprehensive study is done in [27, 28]. The next step is choosing a clear image from the sequence of captured images. A good iris quality assessment based on Fourier spectra analysis was suggested in [9]. After selecting the high-quality image, with morphological image processing operators, the edge of the pupil is determined [29].

A brief overview of the method is as follows:

(i) filling the holes which are pseudocreated by the light reflection on the cornea or further in eye;
(ii) enhancing the contrast of image by adjusting image intensity;
(iii) finding the "regional minima." Regional minima are connected components of pixels with the same intensity value, T, whose external boundary pixels all have a value greater than T;
(iv) applying morphological operators. The operation is repeated until the image no longer changes and sets a pixel to 1 if five or more pixels in its 3-by-3 neighborhood are 1's; otherwise, it sets the pixel to 0 in a binary image from the previous step;

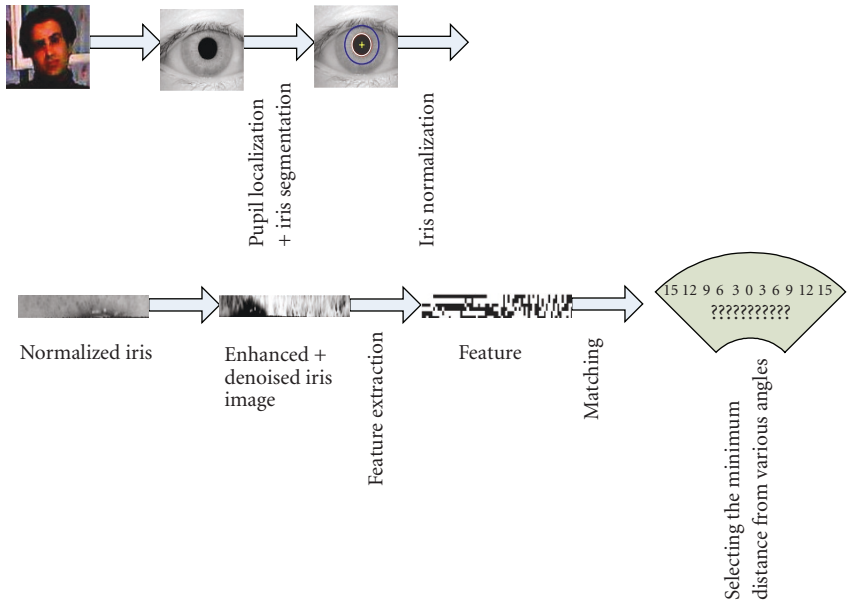

Figure 2: Flowchart of automatic iris recognition system.

(v) removing the small connected parts in image which their areas are less than a threshold.

The pupil now is well detected and its center and radius are gotten. We can also obtain the edge of iris that is mentioned in our previous work [29]. The advantage of this kind of edge detection is its speed and good performance because in morphological processing, we deal with binary images and processing on binary images is very fast. After pupil detection, with trial and error, we get that by choosing an appropriate radius as the outer boundary of iris, the selected region by this threshold contains the collarette structure well. Preprocessing on the selected iris region is the next step that includes iris normalization, iris image enhancement and denoising.

3. IMAGE PREPROCESSING

This step contains three substages. A captured image contains not only the iris but also some parts such as eyelid, eyelash, pupil, and sclera which are not desirable. Distance between camera and eye and environmental light conditions (dilation of pupil) can influence the size of the iris. Therefore, before the feature extraction step, the image must be preprocessed to overcome these problems. These substages are as follows. In our system, we use 320×280 grayscale images.

3.1. *Iris localization*

Iris boundaries can be supposed as two nonconcentric circles. We must determine the inner and outer boundaries with their relevant radius and centers. Several approaches concerning iris edge detection were proposed. Our method is based on iris localization by using image morphological operators and suitable threshold [29]. The summary method is as follows:

(i) evaluating the complement of the image (the absolute subtraction of each pixel's intensity from 255);

(ii) filling holes in the intensity image. A hole is an area of dark pixels surrounded by lighter pixels. We used 4-connected background neighbors for input images which mean a neighborhood whose neighbors are touching the central element on an $(N-1)$-dimensional surface, for the N-dimensional case $(N = 2)$;

(iii) evaluating again the complement of the processed image;

The pupil edge detection is obtained from the preprocessed iris image in the above process. By a suitable threshold and the strategy stated below, the edge of pupil is detected.

(i) Select two appropriate numbers for upper and lower thresholds L, U. L (in the range of $[0\ \ 1]$) determines the detected circle quality. If the parameter L increases to 1, the quality of detected circle decreases and vice versa. U is adjusted to reject small points as a circle. If U increases (from 1 to infinity), only the large circle will be detected and for acceptance all points as a circle, it must be adjusted to 1.

(ii) For $K = 1$ iteration number, do as follows:

  (1) see the intensity of each pixel, if it is lower than $L+K$, convert it to 0 and if it is bigger than $U-K$, covert it to 255;

  (2) otherwise, filter the intensity to the lower one by a scaling factor.

(iii) The processed image is converted to a logical image which means that a black-and-white-type image will be obtained.

For the pupil, in edge detection via morphology operators, maybe some other parts have been detected. Hence, these artifacts must be detected and withdrawn by the process. The algorithm of computing coordinates and radiuses of the resulted image is as follows:

(i) performing morphological operations (clean, spur, and fill) on binary image to remove the mentioned artifacts;

(ii) labeling the connected components of the image ($\mathbf{n}$) in the above step. Repeat the below process from $i = 1n$ times to locate circles among the components:

(1) find the labeled image's pixels that are equal to i. Determine the size of the found component,

(2) conceptually, a square is located around each component, and then the closed feature is compared with a circle occupying the surrounded square,

(3) if it can satisfy the conditions of similarity to a circle, then the feature that is surrounded by square is labeled as a circle. These conditions are related to thresholds L and U, the comparison between obtained component and the circle which can be surrounded by the square, and comparison of the ratio of row against column pixels with a threshold,

(4) the coordinate and radius of the obtained circle are calculated easily by the size of the located square.

As mentioned earlier, after pupil edge detection (inner boundary), the outer boundary is the edge of a circle with a radius of $r_i = 28 + r_p$. In our second algorithm, the edge of a circle with a radius of $r_i = 38 + r_p$ is captured and the lower part of this circle is our desired region. With trial and error, we get that by choosing a radius of 28 pixels from the edge of the pupil, the selected region usually contains the collarette structure well. This region has abundant features of iris opposite to the other parts.

3.2. Iris normalization

Different image acquisition conditions influence and disturb the process of identification. The dimensional incongruities between eye images are mostly due to the stretching of the iris caused by pupil expansion/ contraction from variation of the illuminations and other factors. Other circumstances include variance of camera and eye distance, rotation of the camera or head. Hence, a solution must be contrived to remove these deformations. The normalization process projects iris region into a constant-dimensional ribbon so that two images of the same iris under different conditions have characteristic features at the same spatial location. Daugman [6, 7, 30] suggested a normal Cartesian-to-polar transform that remaps each pixel in the iris area into a pair of polar coordinates (r, θ), where r and θ are on the intervals $[0\ \ 1]$ and $[0\ \ 2\pi]$, respectively. This unwrapping is formulated as follows:

$$I(x(r,\theta), y(r,\theta)) \longrightarrow I(r,\theta) \tag{1}$$

such that

$$\begin{aligned} x(r,\theta) &= (1-r)x_p(\theta) + rx_l(\theta), \\ y(r,\theta) &= (1-r)y_p(\theta) + ry_l(\theta), \end{aligned} \tag{2}$$

where $I(x, y)$, (x, y), (r, θ), (x_p, y_p), (x_i, y_i) are the iris region, Cartesian coordinates, corresponding polar coordinates, coordinates of the pupil, and iris boundaries along the θ direction, respectively. This representation (the rubber sheet model) removes the above-mentioned deformations. We performed this method for normalization and selected 64 pixels along r and 512 pixels along θ and got a 512×64 unwrapped strip. On account of asymmetry of pupil (not being a circle perfectly) and probability of overlapping outer boundaries with sclera or eyelids in some cases and due to the safely chosen radius around the pupil, in the second algorithm we select 3 to 50 pixels from 64 pixels along r and 257 to 512 pixels from 512 pixels along θ in unwrapped iris. The normalization not only reduces exactly the distortion of the iris caused by pupil movement, but also simplifies subsequent processing.

3.3. Iris denoising and enhancement

On account of imaging conditions and situations of light sources, the normalized iris image does not have an appropriate quality. These factors may affect the performance of feature extraction and matching processes. Hence for getting a uniform distributed illumination and better contrast in iris image, we first equalize the intensity of pixels in unwrapped iris image and then filter it with an adaptive lowpass Wiener2D filter to remove high-frequency noises. Wiener2D is a lowpass filter that filters an intensity image which has been degraded by constant power additive noise. It uses a pixelwise adaptive Wiener method based on statistics estimated from a local neighborhood of each pixel. In our method, the size of neighborhoods is 5×5. Wiener2D estimates the local mean and variance around each pixel as follows:

$$\begin{aligned} \mu &= \frac{1}{MN} \sum_{n_1, n_2 \in \eta} a(n_1, n_2), \\ \sigma^2 &= \frac{1}{MN} \sum_{n_1, n_2 \in \eta} a^2(n_1, n_2) - \mu^2, \end{aligned} \tag{3}$$

where η is the N-by-M local neighborhood of each pixel in the image. The filter then creates a pixelwise Wiener filter using the following estimates:

$$b(n_1, n_2) = \mu + \frac{\sigma^2 - \nu^2}{\sigma^2}(a(n_1, n_2) - \mu), \tag{4}$$

where ν^2 is the noise variance. If the noise variance is not given, it uses the average of all the local estimated variances. In the first mode, we used all of the projected iris area and in the second mode, the right part of the unwrapped iris which indicates the lower part of segmented iris is used. The whole preprocessing stages for the two algorithms are depicted in Figures 3 and 4, respectively.

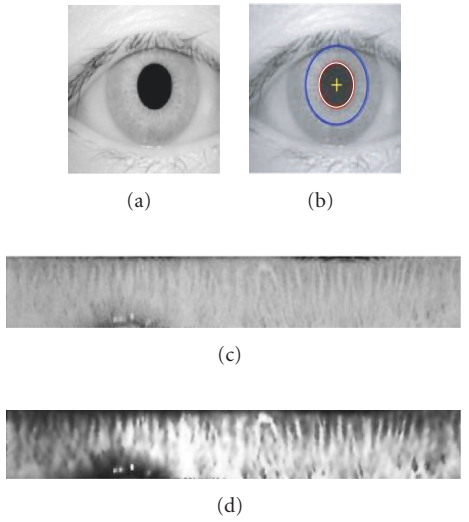

Figure 3: (a) Original image; (b) localized iris; (c) normalized iris; and (d) enhanced iris.

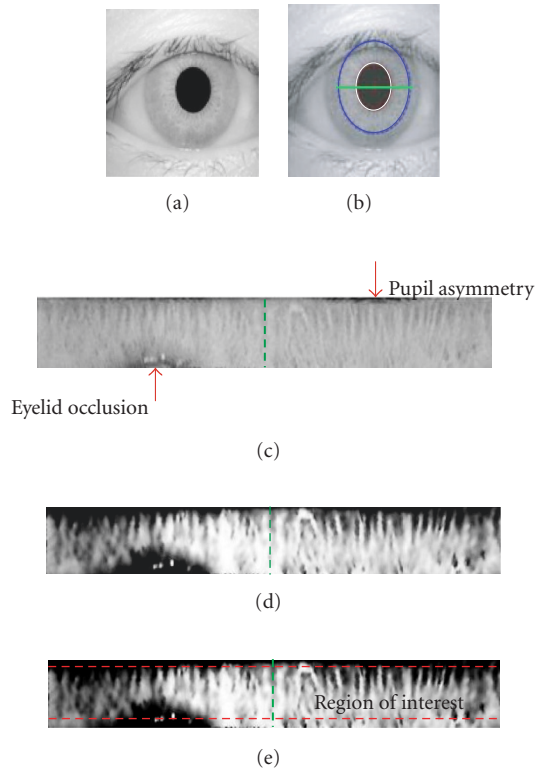

Figure 4: (a) Original image; (b) localized iris; (c) normalized iris; (d) enhanced iris; and (e) region of interest.

4. FEATURE EXTRACTION

The most important step in automatic iris recognition is the ability of extracting some unique attributes from iris which help to generate a specific code for each individual. Gabor and wavelet transforms are typically used for analyzing the human iris patterns and extracting features from them [6–10, 14, 30].

In our earlier work [31], which we have used all iris regions (may contain eyelid/eyelash), wavelet Daubechies2 have been applied to iris. Now by new segmentation of the iris region as mentioned above, we applied the same wavelet. The results show that on account of not including the useless regions in the limited iris boundary, the identification rate is improved well. In Figure 5(a), a conceptual chart of basic decomposition steps for images is depicted. The approximation coefficients matrix cA and details coefficients matrices cH, cV, and cD (horizontal, vertical, and diagonal, resp.) obtained by wavelet decomposition of the input image are shown in Figure 5(b). The definitions used in the chart are as follows.

(i) $C \downarrow$ denote downsample columns—keep the even-indexed columns.
(ii) $D \downarrow$ denote downsample rows—keep the even-indexed rows.
(iii) Lowpass_D denotes the decomposition lowpass filter.
(iv) Highpass_D denotes the decomposition highpass filter.
(v) The blocks under "Rows" convolve with filter of block the rows of entry.
(vi) The blocks under "Columns" convolve with filter of block the columns of entry.
(vii) I_i denotes the input image.

In the first algorithm, we got the 4-level wavelet decomposition details and approximation coefficients of unwrapped iris image and in the second one, the 3-level was chosen. Since our unwrapped image has a size of 512×64 (256×48) pixels, after 4(3) times decompositions, the size of last part is 6×34 (8×34). We arranged our feature vector by combining $408 = ([6 \times 34 \;\; 6 \times 34])$ features in the LH and HL of level-4 (vertical and horizontal approximation coefficients $[LH_4 \;\; HL_4]$) in the first algorithm and $544 = ([8 \times 34 \;\; 8 \times 34])$ in the second algorithm. Then based on the sign of each entry, we assign +1 to the positive entry of feature vector and 0 to others. Finally, we built a 408(544) binary feature vector (FV). The two typical feature vectors are shown in Figure 6.

5. CLASSIFICATION

In classification stage, by comparing the similarity between corresponding feature vectors of two irises, we can determine whether they are from the same class or not. Since the feature vector is binary, the matching process will be fast and simple accordingly. We perform two classifiers based on minimum Hamming distance (MHD):

$$\mathrm{HD} = \mathrm{XOR}\ (\mathrm{codeA}, \mathrm{codeB}), \tag{5}$$

where codeA and codeB are the templates of two images. It is desirable to obtain an iris representation invariant to translation, scale, and rotation. In our algorithm, translation and scale invariance are achieved by normalizing the

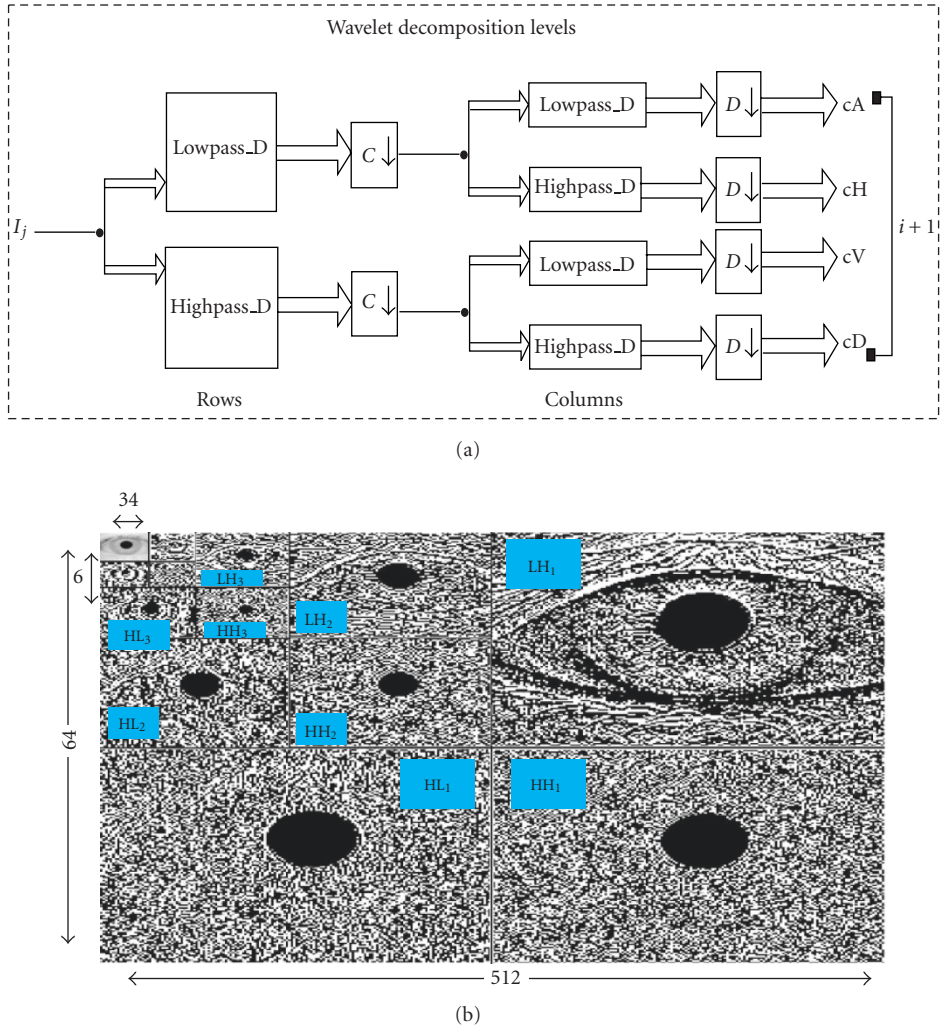

FIGURE 5: (a) Wavelet decomposition steps diagram and (b) 4-level decomposition of a typical image with a db2 wavelet.

FIGURE 6: Two typical feature vectors (a) in the first algorithm with the size of 408 and (b) in the second algorithm with the size of 1088.

original image at the preprocessing step. Most rotation invariance methods which are suggested in related papers are achieved by rotating the feature vector before matching [6, 7, 12, 13, 17, 30], and Wildes did it by registering the input image with the model before feature extraction [11]. Since features in our method are the selected coefficients of decomposition levels which are gotten via wavelet, there is no explicit relation between features and the original image. Therefore, rotation in the original image corresponds to translation in the normalized image [8, 9, 16]. We obtain approximate rotation invariance by unwrapping to different initial angles. Considering that the eye rotation is not very large in practical applications, these initial angle values are chosen from -15° to 15° with steps of three degrees. This means that we define eleven templates which denote the eleven rotation angles for each iris class in the database. Matching the input feature vector with the templates of an iris class means that the minima of these eleven distances are selected as the result. When an iris image is captured in system, the designed classifier compares it with the whole images in each class (depending on the total images for every one). The Hamming distances (HDs) between input image and images in each class are calculated then two different classifiers are being applied as follows.

(i) In the first classifier, the minimum HD between input iris code and codes of each class is computed as follows:

Table 2: Results of illumination test conditions.

Increasing	25	40	60	70	60	80	90	95
Changes in increasing	No	No	No	No	No	No	1 fails	3 fails
Decreasing	25	40	60	70	100	120	130	—
Changes in decreasing	No	No	No	No	No	1 fails	5 fails	—

(1) for each image of class, the HDs between input code and its eleven related codes are computed. Finally the minimum of them is recorded;
(2) if we have n images in each class, the minimum of these n HDs is assigned to the class.

(ii) In the second classifier, the harmonic mean of the n HDs which have been recorded yet is assigned to the class. The harmonic mean formula is as follows:

$$\mathrm{HM} = \frac{\mathrm{length(code)}}{\sum_{i=1}^{\mathrm{length(code)}} (1/\mathrm{code(i)})}. \quad (6)$$

Accordingly, when we sort the results of two classifiers in an ascending order, each class is labeled with its related distance and we call them SHD and SHM, respectively. Even if one of the first two numbers of SHD or SHM denotes to correct class, the goal is achieved. It will be correct if the number is less that the threshold which will be selected based on the overlap of the FAR and FRR plots. Input iris images after coding are compared with all iris codes which exist in database. *Identification* and *verification* modes are two main goals of every security system based on the needs of the environment. In the verification stage, the system checks if the user data that was entered is correct or not (e.g., username and password) but in the identification stage, the system tries to discover who the subject is without any input information. Hence, *verification* is a one-to-one search but *identification* is a one-to-many comparison. This system has been tested in both modes.

6. SENSITIVITY ANALYSIS

As mentioned above by normalizing iris images, scale and size invariant are obtained but other factors can influence the system process. We performed on the second method (half-eye) the sensitivity analysis with three major of them which will be detailed as follows. The input images are the same as in the experimental results and the method of classification is the same as the proposed algorithm, too.

6.1. Illumination

Due to the position of light sources in the various image capturing conditions, the brightness of images may be changed. These changes can damage the process of recognition if feature extraction has a high correlation with them. We performed some various conditions. The test conditions are shown in Table 2. By increasing (decreasing) the brightness of iris region and testing these deformed images as an input to the system and calculating their distances, it was achieved that our feature extraction is a highly illumination invariant. Figures 7(a) and 7(b) show the effect of variance of illumination on distance in two increasing and decreasing ways.

6.2. Contrast

Based on the distribution of image intensities, the contrast of picture is variable. It seems that contrast may be an important factor for the process of recognition. We tested some modes by varying the iris region contrast so that the intensity of an input image was lower than the original image. The results showed that our feature extraction is highly robust versus the variation of contrast. Figure 8(a) represents effect of variance of contrast on the distance of a matching process. Typically for an input iris image, the bounds of histogram for five testing image conditions are shown in Figure 8(b).

6.3. Noise

A fundamental factor which must be considered to design any system is the effect of environment's noises on efficiency of system. Due to the subject of security, being noise invariant is crucial. We have tested two kinds of noises in two different modes. The first mode is applying noise to all images by constant variance and checking identification process. The second mode is applying variable noise for every input image. In the second mode, each image is affected by noise with different characteristics which this mode includes various kinds of alike class noise. Gaussian and Salt and Pepper noises are considered for testing because Gaussian is a popular noise for testing the robustness of most systems and Salt and Pepper noise is composed of random pixels which can destroy the iris region by inserting the black or white pixels and it is the extreme mode of altering. In the Gaussian mode, we created noise by multiplying a constant by a random function and increased the constant in each trial from 0 to 10 with step size equal to 2 and repeated this five times due to the randomness of noise. We get that until constant less than 6, there is no false more than usual conditions but when increased to 8 and 10, the number of added fails increased linearly.

In Salt and Pepper mode, although this kind of noises seriously damage the image, experiments showed that recognition success rate did not change more. It means that by increasing the noise area from 0% to 10% of the whole iris region (randomly 50% Salt and 50% Pepper), in average 3 fails for less than 0.06 and the maximum 8 fails for the added noise with the variance of 0.1 taking place. In Figures 9(a) and 9(b), the performance of verification in two noisy conditions are shown.

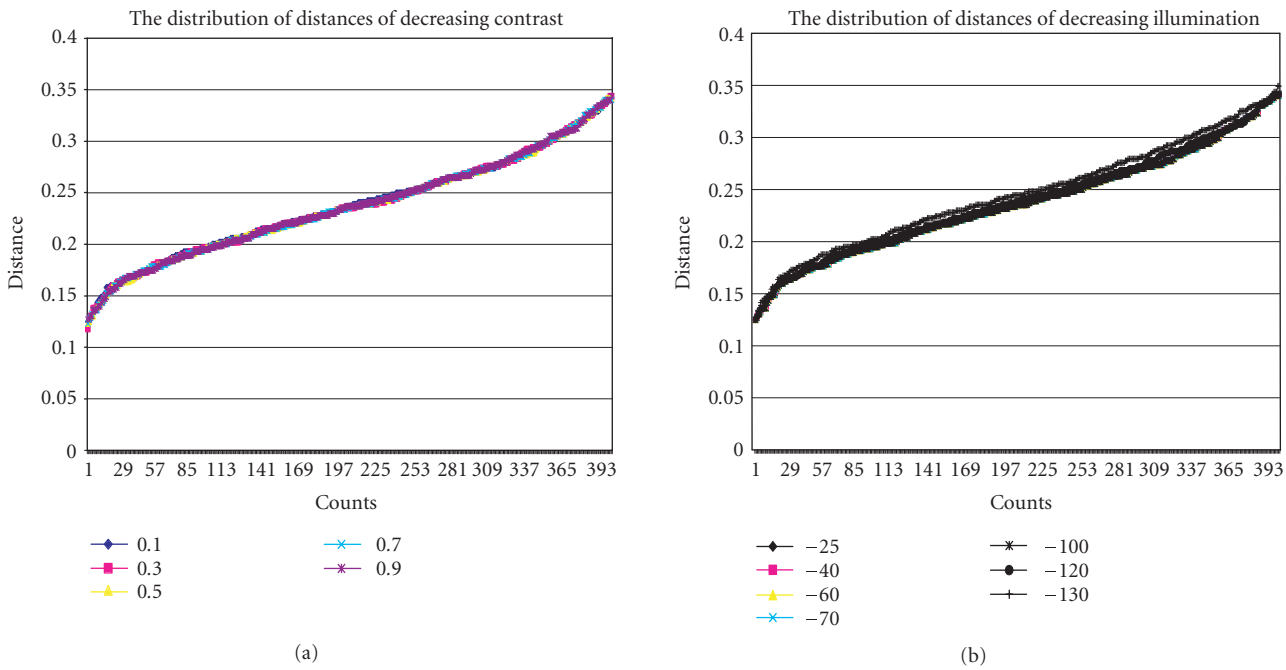

Figure 7: The results of the illumination changing: (a) increasing and (b) decreasing. The upper bounds of increased (decreased) test conditions do not exceed the maximum tradeoff threshold.

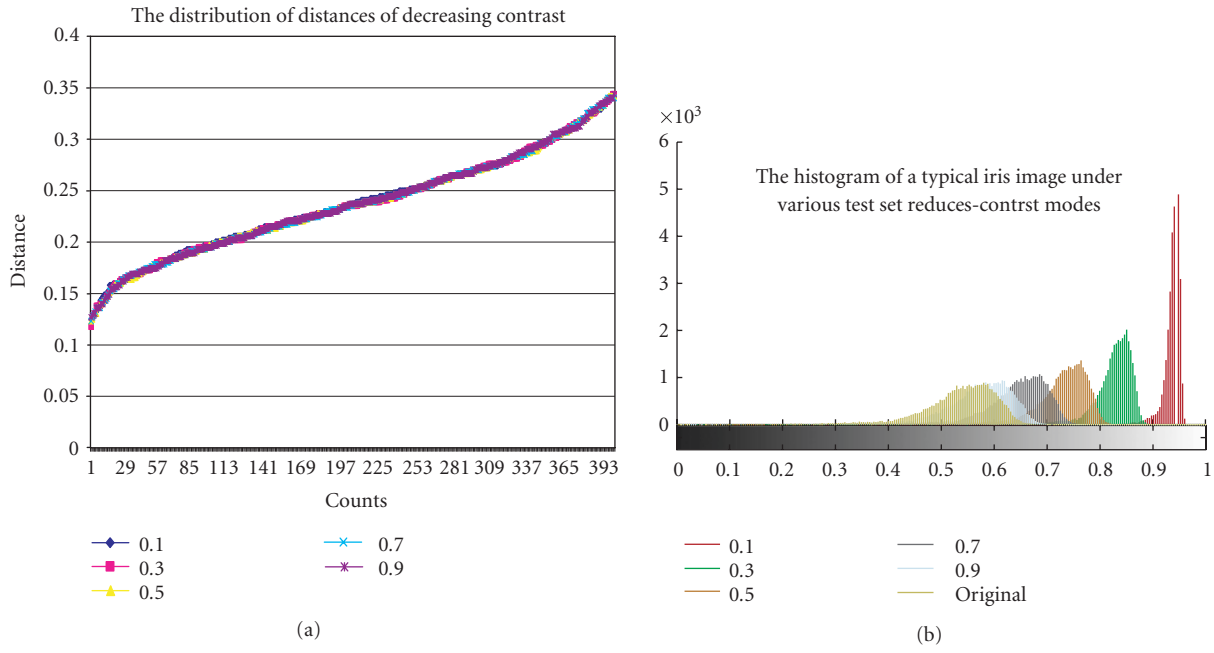

Figure 8: (a) The result of the contsrat changing and (b) the bounds of five test conditions in contrast reduction for a typically sample image.

7. EXPERIMENTAL RESULTS

To evaluate the performance of the proposed algorithm, we tested our alghoritm on CASIA version 1 database. Unlike fingerprints and face, there is no reasonably sized public-domain iris database. The Chinese Academy of Sciences, Institute of Automation (CASIA) eye image database [32] contains 756 greyscale eye images with 108 unique is not clear we recommend to have this figure printed in colors, in which case the authors or their eyes or classes and 7 different images of each unique eye. Images from each class are taken from two sessions with one month interval between sessions. The images were captured [10] specially for iris recognition research using specialized digital optics—

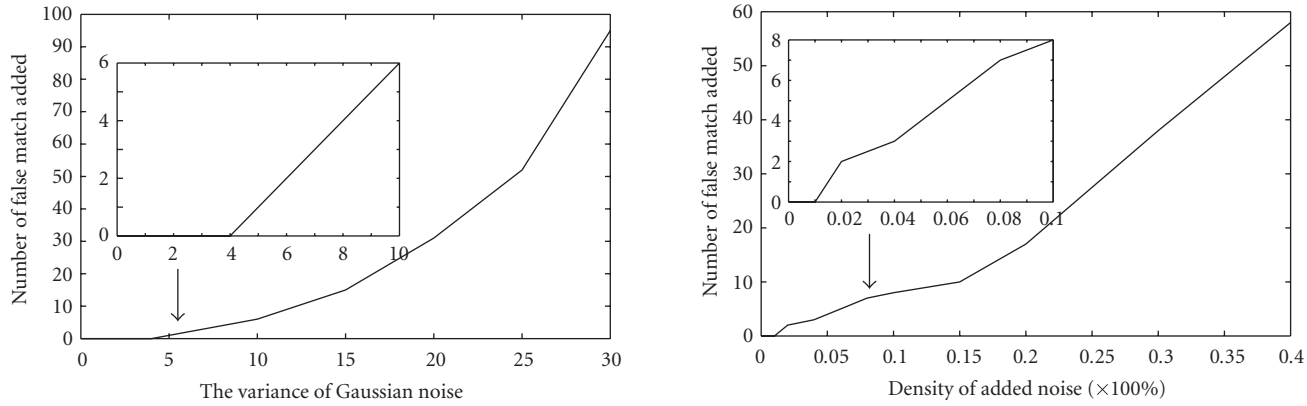

FIGURE 9: The performance of system under two kinds of noises: (a) the result of Gaussian noise adding and (b) the result of Salt & pepper noise adding. The results showed that under the reasonable noisy conditions, the captured images will be recognized well with a little bit smaller success rate.

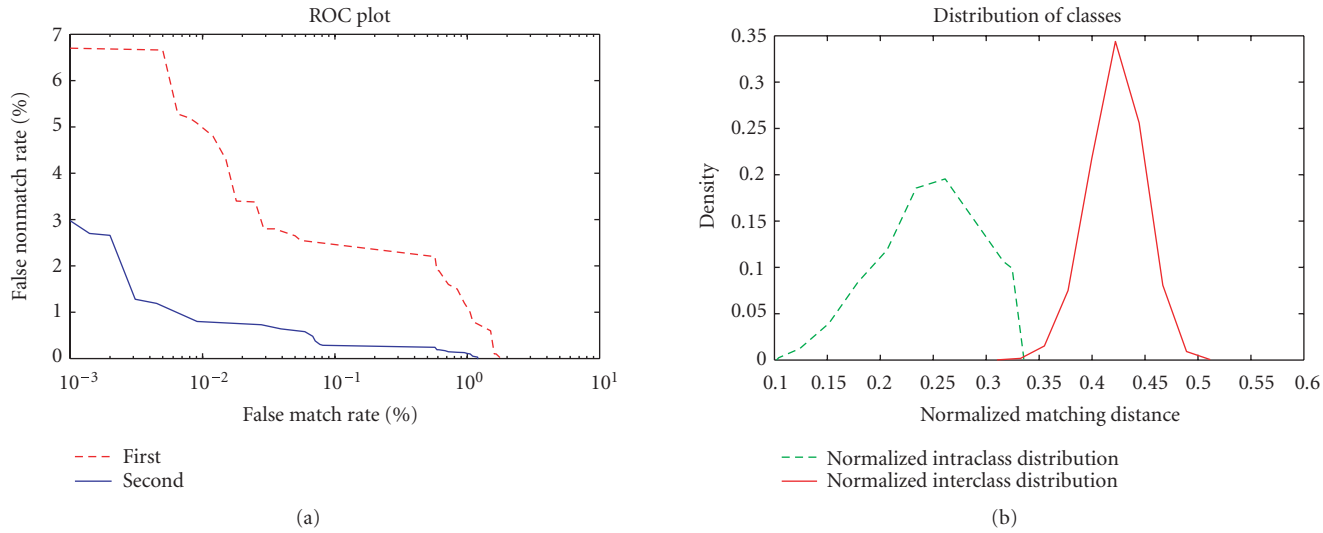

FIGURE 10: (a) The verification results of two proposed methods and (b) the distribution of intraclass and interclass distances. The fewer overlap results, the better recognition results.

a homemade digital camera which used to capture the iris database—developed by the National Laboratory of Pattern Recognition, China. The eye images are mainly from persons of Asian decent, whose eyes are characterized by irises that are densely pigmented, and with dark eyelashes. Due to specialized imaging conditions using near-infrared light, features in the iris region are highly visible and there is good contrast between pupil, iris, and sclera regions. For each iris class, we choose three samples taken at the first session for training and all samples captured at the second session serve as test samples. This is also consistent with the widely accepted standard for biometrics algorithm testing [33, 34].

We tested the proposed algorithms in two modes: (1) identification and (2) verification. In identification tests, an average correct classification rate of the first algorithm was 97.22% and 99.31% was achieved in the second algorithm. The verification results are shown in Figure 10(a) which is the ROC curve of the proposed method. It is the false nonmatch rate (FNMR) versus false match rate (FMR) curve which measures the accuracy of the iris matching process and shows the overall performance of an algorithm. Points in this curve denote all the possible system operating states in different tradeoffs. The EER is the point where the false match rate and the false nonmatch rate are equal in value. The smaller the EER (which is dependent directly on FMR and FNMR and its smaller value with regard to the smaller values of FMR and FNMR intersection) is, the better the algorithm is [16]. EER is about 1.0334% and 0.2687 in two suggested methods, respectively. Figure 10(b) shows the distribution of intraclass and interclass matching distances of the second algorithm. Three typical system operating states of the second proposed method are listed in Table 3.

We analyzed the images that failed in the process and realized that all of the images are damaged mainly with

Table 3: Verification results.

False match rate (%)	False nonmatch rate (%)
0.001	2.98
0.01	0.794
0.1	0.2808

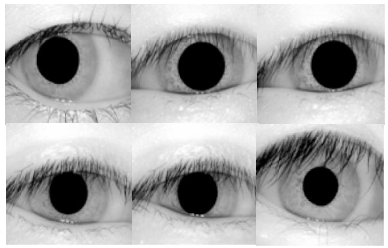

Figure 11: Some of occluded iris images which are not recognized as correct.

Table 4: Comparison of CRRs and EERs.

Method	Correct recognition rate (%)	Equal error rate (%)
Boles and Boashash [12]	92.64	8.13
Daugman [30]	100	0.08
Ma [35]	99.60	0.29
Ma et al. [16]	100	0.07
Tan et al. [8]	99.19	0.57
Wildes et al. [11]	—	1.76
Proposed	97.22	1.0334
	99.31	0.2687

eyelid/eyelash occlusion. If we can detect and withdraw these kinds of occluded images in the imaging phase, the success rate will be improved well. (Unfortunately, we have not collected our database yet and there is no other way except using shared database.) However, with the improvement of iris imaging, such cases can be reduced. Figure 11 shows some of these kinds of images. Table 4 [14] shows the comparison between the various known methods on CAISA iris database and our method has a reasonable and good range in both CCR and EER.

8. CONCLUSIONS

In this paper, we described an iris recognition algorithm using wavelet-based texture features. The feature vector was thresholded to a binary one, reducing the processing time and space, while maintaining the recognition rate. A circular area around the pupil was used in the first iris detection method; while in the second method, the area bounded by the pupil and the lower half of an appropriate circle was utilized. These areas contain the complex and abundant texture information which are useful for feature extraction. Not being engaged with the accurate iris boundary detection, which is a time-consuming process in iris recognition, is one of the advantages of the proposed algorithms. The latter method was successful in coping with partial occlusion of the upper part of the eye, which often happens due to eyelid and eyelashes.

Experimental results using CASIA database showed that relying on a smaller but more reliable part of the iris, although reduced the net amount of information, improved the recognition performance. Sensitivity of the proposed algorithms was examined against contrast, and illumination variation, as well as noise, where the second method proved to be more robust.

REFERENCES

[1] A. K. Jain, R. Bolle, and S. Pankanti, Eds., *Biometrics: Personal Identification in Networked Society*, Kluwer Academic, Dordrecht, The Netherlands, 1999.

[2] D. Zhang, *Automated Biometrics: Technologies and Systems*, Kluwer Academic, Boston, Mass, USA, 2000.

[3] R. P. Wildes, "Iris recognition: an emerging biometric technology," *Proceedings of the IEEE*, vol. 85, no. 9, pp. 1348–1363, 1997.

[4] E. Wolff, *Anatomy of the eye and orbit*, H. K. Lewis, London, UK, 7th edition, 1976.

[5] A. Bertillon, "La Couleur de l'Iris," *Rev. of Science*, vol. 36, no. 3, pp. 65–73, 1885.

[6] J. G. Daugman, "High confidence visual recognition of persons by a test of statistical independence," *IEEE Transactions on Pattern Analysis and Machine Intelligence*, vol. 15, no. 11, pp. 1148–1161, 1993.

[7] J. G. Daugman, "Demodulation by complex-valued wavelets for stochastic pattern recognition," *International Journal of Wavelets, Multiresolution, and Information Processing*, vol. 1, no. 1, pp. 1–17, 2003.

[8] L. Ma, Y. Wang, and T. Tan, "Iris recognition using circular symmetric filters," in *Proceedings of the 16th International Conference on Pattern Recognition*, vol. 2, pp. 414–417, Quebec City, Quebec, Canada, August 2002.

[9] L. Ma, T. Tan, Y. Wang, and D. Zhang, "Personal identification based on iris texture analysis," *IEEE Transactions on Pattern Analysis and Machine Intelligence*, vol. 25, no. 12, pp. 1519–1533, 2003.

[10] L. Ma, Y. Wang, and T. Tan, "Personal iris recognition based on multichannel Gabor filtering," in *Proceedings of the 5th Asian Conference on Computer Vision (ACCV '02)*, Melbourne, Australia, January 2002.

[11] R. P. Wildes, J. C. Asmuth, G. L. Green, et al., "A machine-vision system for iris recognition," *Machine Vision and Applications*, vol. 9, no. 1, pp. 1–8, 1996.

[12] W. Boles and B. Boashash, "A human identification technique using images of the iris and wavelet transform," *IEEE Transactions on Signal Processing*, vol. 46, no. 4, pp. 1085–1088, 1998.

[13] C. Tisse, L. Martin, L. Torres, and M. Robert, "Person identification technique using human iris recognition," in *Proceedings of the 15th International Conference on Vision Interface (VI '02)*, pp. 294–299, Calgary, Canada, May 2002.

[14] S. Lim, K. Lee, O. Byeon, and T. Kim, "Efficient iris recognition through improvement of feature vector and classifier," *ETRI Journal*, vol. 23, no. 2, pp. 61–70, 2001.

[15] K. W. Nam, K. L. Yoon, J. S. Bark, and W. S. Yang, "A feature extraction method for binary iris code construction," in

Proceedings of the 2nd International Conference on Information Technology for Application (ICITA '04), Harbin, China, January 2004.

[16] L. Ma, T. Tan, Y. Wang, and D. Zhang, "Efficient iris recognition by characterizing key local variations," *IEEE Transactions on Image Processing*, vol. 13, no. 6, pp. 739–750, 2004.

[17] R. Sanchez-Reillo and C. Sanchez-Avila, "Iris recognition with low template size," in *Proceedings of the 3rd International Conference on Audio- and Video-Based Biometric Person Authentication (AVBPA '01)*, pp. 324–329, Halmstad, Sweden, June 2001.

[18] C. Sanchez-Avila and R. Sanchez-Reillo, "Iris-based biometric recognition using dyadic wavelet transform," *IEEE Aerospace and Electronic Systems Magazine*, vol. 17, no. 10, pp. 3–6, 2002.

[19] P. Jablonski, R. Szewczyk, Z. Kulesza, A. Napieralski, M. Moreno, and J. Cabestany, "Automatic people identification on the basis of iris pattern image processing and preliminary analysis," in *Proceedings of the 23rd International Conference on Microelectronics (MIEL '02)*, vol. 2, pp. 687–690, Nis, Yugoslavia, May 2002.

[20] R. Szewczyk, P. Jablonski, Z. Kulesza, A. Napieralski, J. Cabestany, and M. Moreno, "Automatic people identification on the basis of iris pattern extraction features and classification," in *Proceedings of the 23rd International Conference on Microelectronics (MIEL '02)*, vol. 2, pp. 691–694, Nis, Yugoslavia, May 2002.

[21] C.-H. Park, J.-J. Lee, M. J. T. Smith, and K.-H. Park, "Iris-based personal authentication using a normalized directional energy feature," in *Proceedings of the 4th International Conference on Audio- and Video-Based Biometric Person Authentication (AVBPA '03)*, pp. 224–232, Guildford, UK, June 2003.

[22] B. V. K. Vijaya Kumar, C. Xie, and J. Thornton, "Iris verification using correlation filters," in *Proceedings of the 4th International Conference on Audio- and Video-Based Biometric Person Authentication (AVBPA '03)*, pp. 697–705, Guildford, UK, June 2003.

[23] K. Bae, S.-I. Noh, and J. Kim, "Iris feature extraction using independent component analysis," in *Proceedings of the 4th International Conference on Audio- and Video-Based Biometric Person Authentication (AVBPA '03)*, pp. 838–844, Guildford, UK, June 2003.

[24] H.-Y. Gu, Y.-T. Zhuang, and Y.-H. Pan, "An iris recognition method based on multi-orientation features and nonsymmetrical SVM," *Journal of Zhejiang University: Science*, vol. 6 A, no. 5, pp. 428–432, 2005, A0505.

[25] A. Poursaberi and B. N. Araabi, "Binary representation of iris patterns for individual identification: sensitivity analysis," in *Proceedings of the 8th International Conference on Pattern Recognition and Information Processing (PRIP '05)*, Minsk, Belarus, May 2005.

[26] A. Poursaberi and B. N. Araabi, "A half-eye wavelet based method for iris recognition," in *Proceedings of the 5th International Conference on Intelligent Systems Design and Applications (ISDA '05)*, Wroclaw, Poland, September 2005.

[27] T. Camus, M. Salganicoff, A. Thomas, and K. Hanna, "Method and apparatus for removal of bright or dark spots by the fusion of multiple images," United States patent no. 6088470, 1998.

[28] J. McHugh, J. Lee, and C. Kuhla, "Handheld iris imaging apparatus and method," United States patent no. 6289103, 1998.

[29] A. Poursaberi and B. N. Araabi, "A fast morphological algorithm for iris detection in eye images," in *Proceedings of the 6th Iranian Conference on Intelligent Systems*, Kerman, Iran, December 2004.

[30] J. Daugman, "Statistical richness of visual phase information: update on recognizing persons by iris patterns," *International Journal of Computer Vision*, vol. 45, no. 1, pp. 25–38, 2001.

[31] A. Poursaberi and B. N. Araabi, "An iris recognition system based on Daubechies's wavelet phase," in *Proceedings of the 6th Iranian Conference on Intelligent Systems*, Kerman, Iran, December 2004.

[32] http://www.sinobiometrics.com/.

[33] T. Mansfield, G. Kelly, D. Chandler, and J. Kane, "Biometric product testing final report," issue 1.0, National Physical Laboratory of UK, 2001.

[34] A. Mansfield and J. Wayman, "Best practice standards for testing and reporting on biometric device performance," National Physical Laboratory of UK, 2002.

[35] L. Ma, "Personal identification based on iris recognition," Ph.D. dissertation, Institute of Automation, Chinese Academy of Sciences, Beijing, China, June 2003.

A. Poursaberi M.S. Graduate of electrical engineering, control branch, Control and Intelligent Processing Center of Excellence, Faculty of Electrical & Computer Engineering, University of Tehran, Iran.

B. N. Araabi received the B.S. degree from Sharif University of Technology, Tehran, Iran, the M.S. degree from University of Tehran, Iran, and the Ph.D. degree from Texas A & M University, Tex, USA, in 1992, 1996, and 2001, respectively, all in electrical engineering. In January 2002, he joined the Department of Electrical and Computer Engineering, University of Tehran, as an Assistant Professor. He is also a Research Scientist at School of Cognitive Sciences, Institute for Studies in Theoretical Physics and Mathematics, Tehran, Iran. He is the author or coauthor of more than 60 international journal and conference publications in his research areas, which include pattern recognition, machine vision, decision making under uncertainty, neurofuzzy systems, cooperative reinforcement learning in multiagent systems, predictive control, fault diagnosis, prediction, and system identification.